J Muscle Res Cell Motil (2007) 28:123–139
DOI 10.1007/s10974-007-9110-0

ORIGINAL PAPER

Comparison of the tension responses to ramp shortening and lengthening in intact mammalian muscle fibres: crossbridge and non-crossbridge contributions

H. Roots · G. W. Offer · K. W. Ranatunga

Received: 23 February 2007 / Accepted: 29 May 2007 / Published online: 4 July 2007

Abstract We examined the tension responses to ramp shortening and lengthening over a range of velocities (0.1–5 L_0/s) and at 20°C and 30°C in tetanized intact fibre bundles from a rat fast (flexor hallucis brevis) muscle; fibre length (L_0) was 2.2 mm and sarcomere length ~2.5 μm. The tension change during ramp releases as well as ramp stretches showed an early transition (often appearing as an inflection) at 1–4 ms; the tension change at this transition and the length change at which it occurred increased with velocity. A second transition, indicated by a more gradual reduction in slope, occurred when the length had changed by 14–28 nm per half-sarcomere; the tension at this transition increased with lengthening velocity towards a plateau and it decreased with shortening velocity towards zero tension. The velocity dependence of the time to the transitions and the length change at the transitions showed some asymmetries between shortening and lengthening. Based on analyses of the velocity dependence of the tension and modelling, we propose that the first transition reflects the tension change associated with the crossbridge power stroke in shortening, or with the reversal of the power stroke in lengthening. Modelling shows that the reduction in slope at the second transition occurs when most of the crossbridges (myosin heads) that were attached at the start of the ramp become detached. After the second transition, the tension reaches a steady level in the model whereas the tension continues to increase during lengthening and continues to decrease during shortening in the experiments; this continuous tension change is seen at a wide range of initial sarcomere lengths and when active force is reduced by the myosin inhibitor, BTS. The continuous tension decline during shortening is not abolished by caffeine, but the rate of decline is reduced when the active force is depressed by BTS. We propose that stiffening of non-crossbridge visco-elastic elements upon activation contributes to the continuous tension rise during lengthening and the release of such tension and Ca-insensitive deactivation contribute to the tension decline during shortening in muscle fibres.

Keywords Force–velocity relations · Power stroke · Caffeine · BTS · Modelling · Crossbridge cycle

H. Roots · G. W. Offer · K. W. Ranatunga (✉)
Muscle Contraction Group, Department of Physiology, School of Medical Sciences, University of Bristol, Bristol BS8 1TD, UK
e-mail: k.w.ranatunga@bristol.ac.uk

Introduction

The force that a muscle develops declines with shortening velocity reaching zero at the maximum velocity (V_{max}); the maximal mechanical power output occurs at some intermediate velocity (0.2–0.4 V_{max}). This shortening limb of the force–velocity (F–V) relation is typically examined using the isotonic release (or force step or load clamp) method (Jewell and Wilkie 1958; Edman et al. 1976); an active muscle developing isometric plateau force (P_0) is suddenly made to shorten against different loads of $<P_0$ and the steady velocity, after the initial rapid phase, is measured. In contrast, the lengthening limb of the F–V relation is usually determined by the isovelocity method, recording the force response to ramp stretches of different velocities (Edman et al. 1978, 1981, 1982; Flitney and Hirst 1978; Lombardi and Piazzesi 1990; Månsson 1994; Piazzesi et al. 1992; Stienen et al. 1992). An active muscle develops ~$2 \times P_0$, and stores energy, as lengthening velocity is increased to 1–2 L_0 (muscle fibre length)/s.

Recently, we reported that the force response during a ramp stretch shows an early change in slope (the P_1 transition) followed by a later, more gradual change in slope (the P_2 transition) both attributed to crossbridge characteristics (Pinniger et al. 2006). The P_1 transition was thought to arise from the reversal of the power-stroke in the attached post-stroke crossbridges, while the P_2 transition marked the change to a new steady-state indicated by the detachment of all the original attached crossbridges. After the P_2 transition, the tension continued to rise and this was attributed to continuing stretch of non-crossbridge elements (Edman and Tsuchiya 1996; Pinniger et al. 2006). Pertinently, Ford et al. (1977) and Bressler (1985) observed, in the tension response to ramp *shortening* in frog muscle fibres, an early ''bulge'' or inflection which may be a counterpart to the P_1 transition above. Intriguingly, during ramp shortening of mammalian muscle (see Joyce et al. 1969; Asmussen and Marechal 1989), the tension continues to *decline* (counterpart to the rise in tension during lengthening) after the P_2 transition; however, a systematic examination is lacking and the mechanism of this continued tension decline remains unclear. The continued tension decline was not seen in the controlled-velocity experiments of Cecchi et al. (1978, 1981) on frog fibres.

The primary aim of the present study was fully to characterise the features of the force response during a ramp (isovelocity) length change, particularly during shortening, in maximally activated intact rat muscle fibre bundles. Preliminary results of this study have been reported previously in abstract form (Roots and Ranatunga 2005, 2006).

Methods

Experiments were performed on small bundles of intact muscle fibres isolated from the flexor hallucis brevis (FHB) muscle of adult male rats (250–300 g, body mass) that were humanely killed with an intra-peritoneal injection of an overdose (>200 mg kg^{-1} body mass) of sodium pentobarbitone (Euthatal, Rhône Mérieux). FHB contains a predominance of fast (~90% type 2) fibres (Coupland and Ranatunga 2003). Bundles of 5–10 intact excitable fibres were dissected from the mid-belly of the muscle under dark-field illumination and aluminium foil T-clips were attached to the tendons at either end of the preparation within 0.2 mm of the fibre-ends. The preparation was mounted horizontally between a force transducer (AE 801 element; AME, Horten, Norway) and a servomotor in a flow-through stainless steel chamber (volume ~2 ml). The force transducer had a natural resonant frequency >5 kHz and the servomotor was capable of completing a 5% L_0 length step in <1 ms and >20% L_0 length step at lower velocities. The chamber was perfused at 0.5 ml min^{-1} with a physiological saline solution containing (mM): NaCl, 109; KCl, 5; $MgCl_2$, 1; $CaCl_2$, 4; $NaHCO_3$, 24; NaH_2PO_4, 1; sodium pyruvate, 10 and 200 mg l^{-1} of bovine foetal serum; the solution was continuously bubbled with 95% O_2 and 5% CO_2. In experiments using N-benzyl-*p*-toluene sulphonamide (BTS), a small volume (<1 ml per 100 ml) of BTS dissolved in DMSO was added to the physiological saline solution to obtain 5–10 μM BTS concentrations; the normal saline flow through the chamber was then replaced with BTS saline flow to expose the preparation to BTS. Most experiments were conducted at 20°C, but some also at 30°C; temperature control (±1°C) of the solution was achieved by a Peltier device fitted underneath the chamber and the temperature was monitored with a thermocouple inside the chamber.

Experimental protocol

The preparation was set to an initial length (optimal length, L_0) where isometric tetanic tension was maximal; the sarcomere length using He–Ne laser diffraction for this condition was typically ~2.5 μm. This was approximately as expected from the relationship between steady state tetanic tension and length for rat muscle fibres, where the optimal sarcomere length has been found to be in the range of 2.1–2.5 μm (Elmubarak and Ranatunga 1984; ter Keurs et al. 1984). The mean (±s.e.m.) fibre length (L_0) and width of the fibre bundles were 2.17 (±0.012) mm and 146 (±3.3) μm, respectively (n = 23).

Following an equilibration period of at least 30 min, control isometric tetanic contractions were recorded at L_0. Using platinum plate electrodes the fibre bundles were stimulated at 70–100 Hz to give a steady tetanic tension and ramp shortening/stretches of 5–20% L_0 were applied on the tension plateau (see Fig. 1) at velocities ranging from 0.1 to 10 L_0/s; the duration of tetanic stimulation (500–1000 ms) was adjusted as appropriate for tension recording. In some preparations the change in the relative position of two markers, placed on the surface of the fibre bundle, was monitored using a position-sensitive detector (Hamamatsu Photonics, S3932; see Mutungi and Ranatunga 2001); the two markers (small aluminium foil pieces or human hair) were placed 0.5–0.7 mm apart and on the force transducer half of the bundle, so that the relative displacement of their magnified images provided a signal for the segment-length change (see Fig. 1C).

Each experiment was completed by recording an isometric tetanic contraction at L_0. The mean (±s.e.m.) tetanic tension (P_0) was 187 (±4.3) kN m^{-2} at 20°C (n = 23); as a ratio of the P_0 recorded at the beginning, P_0 at the end of the experiment was 0.87 (±0.007; n = 19, excluding the four BTS experiments where full recovery was slow and not determined).

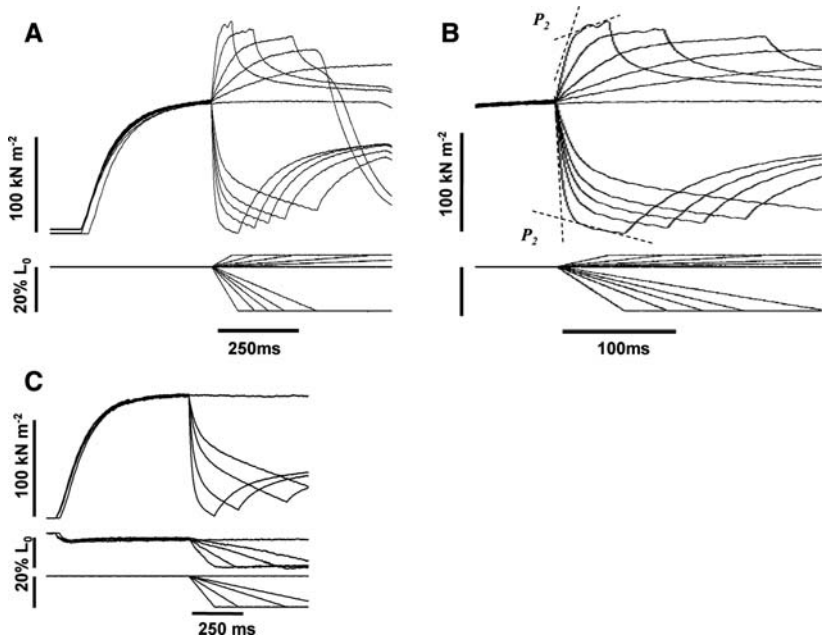

Fig. 1 Tension responses to ramp length changes. **A**: A selection of sample recordings from one preparation at L_0 and 20°C illustrating the tension responses (upper traces) to ramp length steps (lower traces) applied on the plateau of a tetanic contraction; the length step amplitude was 0.05 L_0 for lengthening and 0.2 L_0 for shortening. The duration of tetanic stimulation was shorter in two of the contractions; also shown is an isometric contraction. The tension change to a ramp length step occurs in two phases, an initial fast phase followed by a later slow phase. After completion of the ramp, the tension recovers towards P_0 but the recovery is incomplete. **B**: The same tension traces are shown at an expanded time scale. The tension at the change in slope (P_2 transition) was estimated from the intersection between two straight lines fitted to the tension records (as shown in two records). **C**: Sample recordings from another preparation in which the length change in a short (0.55 mm long) segment of the fibre bundle was also monitored (middle traces) during ramp shortening (lower traces); the separation between two markers placed on the bundle surface, and nearer the force transducer end, was monitored. Note the similarity between the length changes applied to the bundle and the change in segment length and, also, that the segment shortens about 4% during the initial tetanic tension rise

Data recording and analysis

The length and the tension signals from the transducers were collected via a CED 1401 laboratory interface using Signal 2 and Signal 3 software (Cambridge Electronic Design Ltd., Cambridge, UK) and stored on a Personal Computer. Tension and time course measurements were determined offline using Signal software and additional analysis and non-linear curve fitting were performed using Fig P (Biosoft, Durham, USA), Excel (Microsoft) and Prism (GraphPad) software.

Results

General features of the tension response to ramp lengthening and shortening

The superimposed tension traces shown in Fig. 1A illustrate the general features of the tension responses to ramp shortening and lengthening; they were recorded from a preparation at L_0 where the resting muscle tension was minimal. In each recording, the fibre bundle-ends were held isometric until the tension-plateau, P_0, and then a ramp length change at a constant velocity was applied. During a 5% L_0 ramp lengthening, the tension rises rapidly initially and then more slowly until the end of the ramp, as described previously (Pinniger et al. 2006); for convenient description and consistency with previous studies, the point at which this change in slope occurs is referred to as the P_2 transition. After the end of the ramp, the tension recovers incompletely towards P_0 so that there is a residual incremental force (P_3) at the stretched length. Strikingly, an inverse of this tension response is seen during ramp shortening: the tension falls rapidly initially and undergoes a transition (P_2) after which tension declines more slowly till the end of the shortening ramp. After completion of the 20% L_0 ramp shortening, the tension rises to a value less than P_0 indicating a residual force deficit. Figure 1B shows the tension responses on an expanded time scale. The tension level at the P_2 transition was estimated from the point of intersection between two linear regressions fitted to the tension record on either side of the P_2 transition, as done in previous studies on lengthening muscle (see

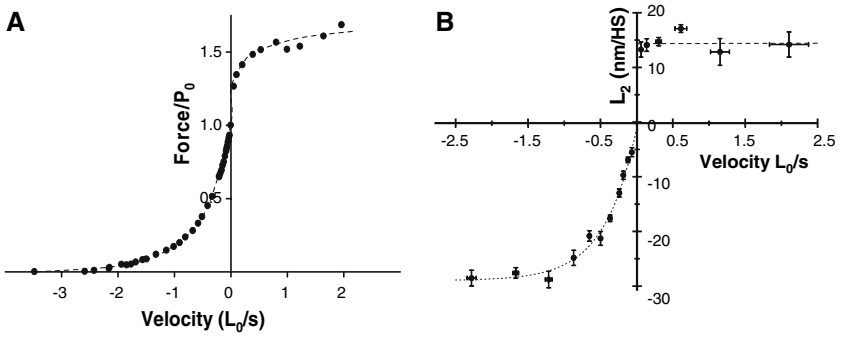

Fig. 2 The P_2 transition and the force–velocity relation. **A**: The muscle tension at the P_2 transition was normalised to P_0 and is plotted against the shortening (negative) velocities and lengthening (positive) velocities. The data are from one fibre bundle at 20°C and the curve is fitted by eye. **B**: L_2, the length change at the P_2 transition, was determined using the ramp length record and is plotted (in nm per half-sarcomere, HS, taken as 1.2 μm) against the velocity. The lines are fitted by eye to the pooled data from 10 fibre bundles where a symbol denotes the mean (±s.e.m.) of ~15 values (total n = 165) for shortening; the data for lengthening are from four of the fibre bundles and a data point represents the average of five values (total n = 30). Note that during lengthening L2 is ~15 nm/HS and, within experimental scatter, it is relatively insensitive to velocity; on the other hand, the magnitude of L_2 increases with shortening velocity to reach a steady (negative) value of ~25–30 nm/HS at velocities above ~1 L_0/s

Pinniger et al. 2006). No detailed analyses were made on the residual force enhancement and the residual force deficit; our particular interest in this study was to characterize features of the tension response *during* a ramp length change, particularly during ramp shortening. Figure 1C shows traces from another experiment where the change in length of a segment of the bundle was also monitored; the segment length change shows a basic similarity with the applied ramp shortening.

The P_2 transition and the force–velocity (F–V) relation

Assuming that the muscle tension at the P_2 transition (estimated as shown in Fig. 1B) represents the crossbridge tension during a constant velocity length change, a F–V relation can be constructed. Figure 2A shows such an F–V relation at 20°C from one preparation. The lengthening limb of the F–V relation is similar to that we previously reported (Pinniger et al. 2006) from the same muscle; the tension increases to ~1.6 P_0 as the velocity is increased above ~1–2 L_0/s. The shortening limb of the F–V relation (F–V_s relation) is similar to that reported previously from rat fast (extensor digitorum longus) muscle, using the isotonic release method (Ranatunga 1984). In those isotonic experiments, however, the data were limited to force levels <0.6 P_0; it can be seen from Fig. 2A that, using the isovelocity approach, a fuller F–V_s relation could be obtained in the present experiments. For comparison, such F–V_s data, from 11 experiments at 20°C and from 3 experiments at 30°C, were analysed using A.V. Hill's (1938) hyperbolic equation; a non-linear curve fitting was made on the force and velocity values without a constraint to pass through P_0. The pooled data for V_{max} and a/P_0 (governing the curvature of the plot) are given in Table 1, along with the data for fast extensor digitorum longus muscle from our previous study (Ranatunga 1984). Although the absolute values are somewhat different, the temperature-dependent changes (i.e. a higher V_{max} and a lower curvature, or higher a/P_0, at 30°C than at 20°C) are similar between the two studies. The lower V_{max} and a/P_0 values in the present study may be

Table 1 Descriptive characteristics of the force–shortening velocity relation of rat fast muscle fibres determined at rest length (L_0) and at two temperatures

	20°C		30°C	
	V_{max} (L_0/s)	a/P_0	V_{max} (L_0/s)	a/P_0
Present study	3.98 (±0.54)	0.141 (±0.012)	8.68 (±0.74)	0.23 (±0.009)
Ranatunga (1984)	4.97 (±0.25)	0.267 (±0.027)	9.82 (±0.46)	0.344 (±0.03)

Note that the present study employed force measurement at P_2 transition during ramp shortening on fibre bundles from fast flexor hallucis brevis (a foot muscle, L_0 ~2 mm), whereas Ranatunga (1984) used steady velocity measurement after isotonic release (i.e. during force-clamp) on fibre bundles from fast extensor digitorum longus (a calf muscle, L_0 ~8–10 mm). V_{max} (maximum shortening velocity) and a/P_0 ratio were obtained from fitting the A.V. Hill (1938) equation to the force and velocity measurements. Each value gives the mean (±s.e.m.): n = 3 at 30°C in the present study and n = 9–11 for others. On the basis of the above data, the maximum filament sliding velocity at physiological temperatures (>30°C) would be >10 μm/s (per HS) for fast mammalian muscle

due to two factors. Firstly, the two muscles have different fast (type-2) fibre type compositions (see Coupland and Ranatunga 2003). Secondly, the tension measured at the P_2 transition during a length ramp has a contribution from the continuous tension change, believed to be from non-crossbridge elements (Pinniger et al. 2006); when the shortening force data from one experiment were approximately corrected for such a contribution, both V_{max} and a/P_0 ratio increased but not enough to fully account for the differences. It would be interesting to employ both isotonic and isovelocity techniques on the same preparation in a future study. In seven of the above experiments at 20°C, the isometric force (P_0*) from extrapolation of the fitted curve to zero velocity was higher than the measured P_0, indicating that the velocity data at higher force levels deviated from the hyperbolic curve. Such a deviation in the F–V relation for shortening was first reported in experiments on frog fibres (Edman 1988) and this feature was recently found also in mouse muscle fibres (Edman 2005).

Figure 2B shows pooled data for the velocity dependence of the length change L_2 at which the P_2 transition occurs. The data shows that L_2 during lengthening, sometimes referred to as the ''critical stretch'', is insensitive to velocity—as reported in many previous studies (see references in Pinniger et al. 2006). Interestingly, Bagni et al. (2005) have shown that, even with fast ramp stretches (>10 L_o/s), where the force declines at or after P_2 during a stretch, L_2 in frog fibres was independent of stretching velocity; L_2 was ~11 nm/HS and it correlated with the mean crossbridge extension. In the present experiments, L_2 is ~1.2% L_0; the mean (±s.e.m.) value for L_2 from 4 preparations (n = 30) was 14.4 (±0.65) nm/HS (half sarcomere = 1.2 μm) at 20°C. To our knowledge, L_2 for shortening has not been characterised before. Our results in Fig. 2B shows that the magnitude of L_2 increases with shortening velocity, up to about 1 L_0/s, and reaches an approximately steady value as the velocity is increased further to ~3 L_0/s; measurement of L_2 was difficult at higher shortening velocities. From 10 experiments, the mean (± s.e.m.) L_2 value for velocities >1 L_0/s, was 28.4 (±0.80, n = 42) nm/HS; this is much higher than that for lengthening.

The P_1 transition

Figure 3 shows the tension response to a ramp shortening, displayed at different scales to highlight another feature of the tension decline. The records illustrate that the P_2

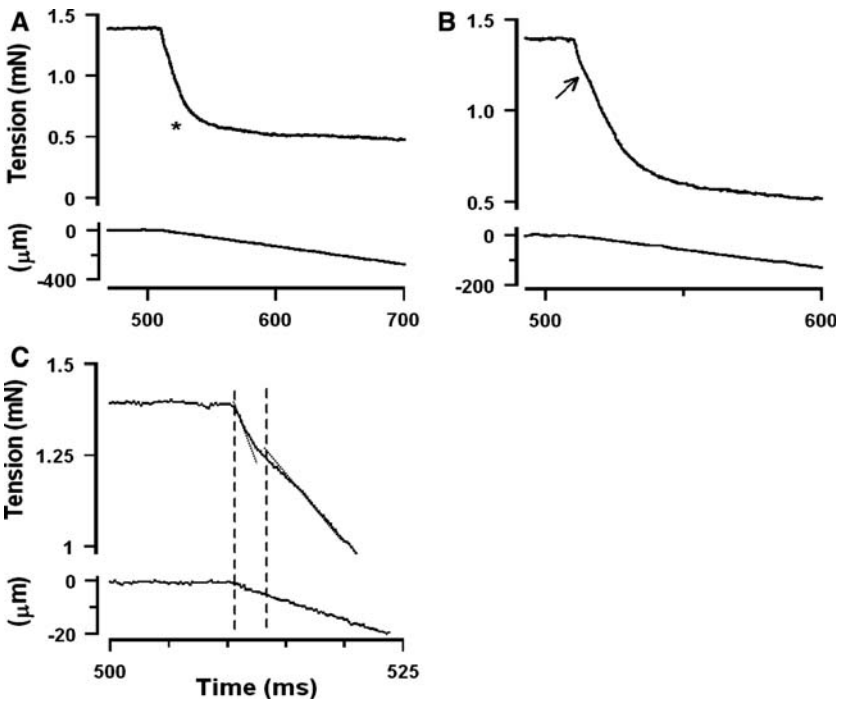

Fig. 3 The P_1 transition. A: A tension trace (upper trace) during a ramp shortening from a tetanus plateau where the asterisk denotes the P_2 transition; the velocity is ~0.7 L_0/s and L_0 ~2.0 mm. Same records are displayed at two different expansions in **B** and **C**. Note that when examined at an expanded time scale (**B**) an early change in slope (P_1 transition, denoted by an arrow) is seen on the tension decline. **C**: The P_1 transition appears as an inflection, where the slope of tension change is initially high, then it decreases and increases again (superimposed dotted lines). The P_1 tension was measured near the midpoint (as in Pinniger et al. 2006), as indicated by the two vertical dashed lines; the corresponding length change (L_1) was determined from the length record

transition (denoted by an asterisk in A) is preceded by an earlier transition (P_1, indicated by an arrow in B). Close inspection revealed that P_1 transition was an inflection (see Fig. 3C); Ford et al. (1977) and Bressler (1985) clearly commented on this feature in frog muscle fibre experiments and we characterised the inverse of this tension change during ramp lengthening in our previous study (Pinniger et al. 2006).

Figure 4A shows the mean (±s.e.m.) data for the amplitude P_1 and the time at which the P_1 transition occurred (as shown in Fig. 3C), for a range of velocities. Despite scatter, the data show that the P_1 amplitude is proportional to velocity during shortening as well as during lengthening. The time to P_1 transition is uncorrelated with lengthening velocity, as found in our previous study (Pinniger et al. 2006); on the other hand, the time to P_1 shows a significant negative correlation with shortening velocity ($P < 0.05$). The length change L_1 at which the P_1 transition occurs was correlated with velocity both during lengthening and shortening ($P < 0.01$); Figure 4B shows L_1 is proportional to velocity in lengthening, whereas L_1 values at different shortening velocities indicate a non-linear curvy distribution (dotted line).

Previously (Pinniger et al. 2006) we showed that the initial slope of the tension rise during ramp lengthening was similar to that obtained from the T_1 tension responses to rapid releases in the same preparation, as described by Huxley and Simmons (1971). We did not measure the initial slope here, but from the ''linear'' slopes of the relations in Fig. 4(A, B), the average stiffness at the P_1 transition was found to be similar for shortening and lengthening, ~50 P_0/L_0. This is somewhat lower than, but in the same range as, the slope of the T_1 tension versus length step amplitude (~65 P_0/L_0) in this preparation at 20°C (Pinniger et al. 2005). All the stiffness values above may be under-estimates because of end-compliance effects and some recovery at P_1.

Tension change after the P_2 transition

In order to characterize this slow continued tension change, the slope of the linear regression fitted to the post-P_2 tension record is plotted (as P_0/s) against velocity in Fig. 5. The rate of tension change after the P_2 transition is directly proportional to velocity during lengthening, or during low velocity shortening; this phase corresponds to a stiffness of ~7 P_0/L_0 which is similar to the value determined for lengthening in the previous study (Pinniger et al. 2006). The slope reaches a limiting value at shortening velocities higher than ~1 L_0/s although the rate could not be determined at velocities approaching V_{max}.

A possible explanation for the continued force decline during ramp shortening is that, at L_2, the sarcomeres had shortened into the ascending limb of the force–length relation, the tension decline being due to a decrease of filament overlap. Taking the resting sarcomere length to be

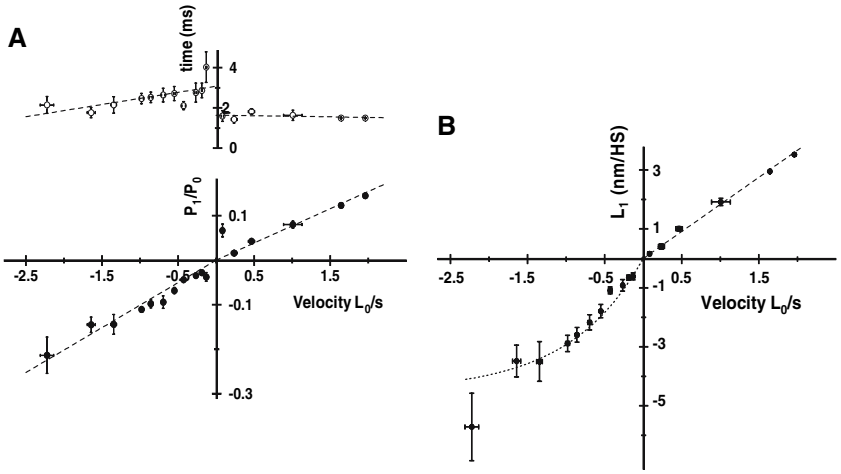

Fig. 4 The velocity dependence of P_1 transition. **A**: (lower panel), Pooled data from 10 fibre bundles show the velocity dependence of the amplitude of P_1 (as a ratio of P_0). For shortening, each symbol represents the mean (±s.e.m.) of 8 values, (total $n = 88$) and for lengthening, each symbol is the mean (±s.e.m.) of 1–3 values (total $n = 14$) from 4 of the 10 fibre bundles. The dotted lines are calculated linear regressions ($P < 0.01$). P_1 increases with increase of velocity during both shortening and lengthening. **A**: (upper panel), With lengthening, the time to the P_1 transition remains approximately constant at ~1–2 ms and shows no correlation ($P > 0.05$) with velocity, as reported previously (see Pinniger et al. 2006): with shortening the time to P_1 decreases with increase of velocity ($P < 0.01$). **B:** The length change L_1 from the beginning of a ramp to the P_1 transition is plotted against the velocity; data for L_1 (pooled as in A) is plotted in nm/HS and are significantly correlated with velocity for both lengthening and shortening ($P < 0.01$). Note that L_1 increases proportionately with velocity during lengthening (dashed line—calculated linear regression); data for shortening indicates a curve (dotted line—fitted by eye)

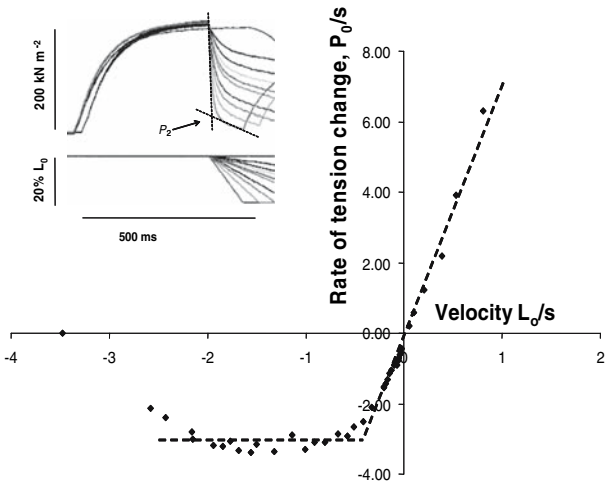

Fig. 5 Tension change after the P_2 transition. (Inset) Tension responses to ramp shortening at a range of velocities from one bundle are superimposed on the isometric tetanus. The rate of tension change after the P_2 transition was calculated from the slope of a linear regression fitted to the post-P_2 tension trace and is plotted as P_0/s against velocity (data at 20°C). Excluding values at higher shortening velocities (>2 L_0/s) where the determination of the post-P_2 slope was difficult, two phases are seen in the data distribution; phase (i), a proportionate dependence on velocity for low shortening velocities that extends to lengthening and (ii), a velocity-independent phase at intermediate shortening velocities

~2.5 μm and assuming up to 5% shortening in the initial tension rise during activation (Fig. 1C; see also Mutungi and Ranatunga 2000) and L_2 of <2%, the sarcomere length at L_2 would be ~2.3 μm; this is not on the ascending limb of the steady state force–length relation (i.e. below ~2.0 μm, see methods). However, at the end of some large shortening steps (up to 20% L_0), the fibres would have shortened into the ascending limb, as can be seen from Fig. 1 (and Fig. 8B) where the redeveloped tension after the fast ramps do not to reach the initial isometric tension level even if the stimulation had been continued. Out of nine preliminary experiments in which the F–V_s relation was examined at approximate L_0, the tension decline was not evident in two preparations (see Roots and Ranatunga 2005), and it remained possible that the initial length setting may have been different in them. In order to address this issue further, we examined in a separate series of experiments, the tension response to ramp shortening (at 1–3 velocities) over a wide range of initial fibre length, covering the ascending limb, the plateau region and the descending limb of the force–length relation.

Sarcomere length dependence of continuous tension decline in ramp shortening

Figure 6(A–D) shows tension traces to ramp shortening at one velocity recorded at 4 different initial fibre lengths; records in A and B, respectively, correspond to the ascending limb and the plateau of the force–length relation; the resting tension was minimal and a continued decline of force after P_2 is seen in both. Figure 6(C, D) shows tension responses on the descending limb of the force–length relation; the resting tension has increased and the (active) isometric force before the ramp is reduced. In these cases the continued tension decline during the shortening ramp is not seen; in C, the post-P_2 tension remains approximately constant and in D, it shows a modest rise. The tension responses during ramp shortening of frog fibres also show a similar rise (positive slope) after the P_2 transition at longer sarcomere length of ~2.6–2.8 μm (see Fig. 10A in Edman and Reggiani 1984 and Fig. 2 in Morgan et al. 1991). It is relevant to note that because of the increased resting tension in C and D, the tension level would have been affected by the decrease of resting tension during ramp shortening. At much longer initial fibre lengths, where the resting tension was even higher, the tension level during the ramp shortening indeed fell to below the initial resting tension level, probably due to hysteresis in the resting tension behaviour.

Figure 6E shows a plot of the data collected from one preparation at a range of initial lengths. The isometric tetanic tension data (filled circles) show the characteristic relation with evidence of 4 linear segments, i.e. a two-segment ascending limb, a plateau and a descending limb. The results are remarkably similar to our previous findings from rat biceps brachii muscle (Elmubarak and Ranatunga 1984) although in that study the sarcomere length was measured after fibre-fixation. Despite the scatter in the tetanic tension data, their distribution is approximately as expected from the overlap between thick (length ~1.6 μm) and thin filaments (length 1.2 μm in the rat; see Elmubarak and Ranatunga 1984; Edman 2005). The resting tension data show a hysteresis and a sharp increase beginning in the length range of the descending limb. Plotted also is the linear slope of the tension record after the P_2 transition (upper panel, right ordinate) during the ramp shortening. The data show that the continued tension decline (a negative slope) is evident when recorded on the ascending limb and on the plateau region; the slope becomes slightly positive only on the descending limb region (sarcomere length >2.8 μm). Except at very long sarcomere length (>3.2 μm) where it was slightly longer, L_2 at this velocity remained approximately constant (~1.5–2% L_0) within a wide range of sarcomere length (P>0.1). Similar experimental data were obtained in two other experiments. Given that L_2 is <2.5% L_0, these findings do not suggest that the continued tension decline after P_2 at L_0 can be accounted for by a decrease of filament overlap during shortening.

In two experiments, we examined the tension response to both ramp stretch and shortening (~0.7 L_0/s, amplitude

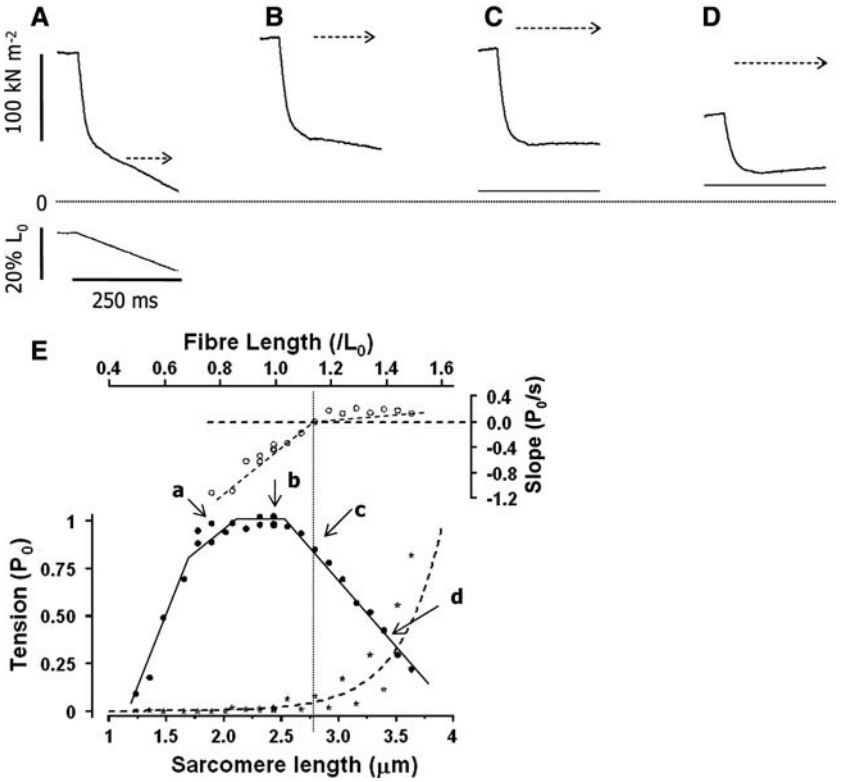

Fig. 6 Dependence of the tension decline on fibre length. **A**, **B**, **C**, **D**: Sample tension responses to ramp shortening at 0.73 L_0/s (length trace is shown in A—lower panel) recorded at four different initial lengths from one preparation; the passive/resting tension is already subtracted from the responses. The initial sarcomere lengths were 1.90 μm (**A**), 2.44 μm (**B**), 2.80 μm (**C**) and 3.40 μm (**D**) and are labelled as a, b, c and d in **E**. The zero tension level is indicated by the horizontal dotted line and the resting fibre tension by the solid horizontal lines below the tension records in **C** and **D**; resting tension was near zero in **A** and **B**. The horizontal arrows in each frame denote approximately the expected isometric tension due to change of filament overlap resulting from a 20% L_0 shortening (~0. 5 μm in a sarcomere). **E**: The resting tension (star symbols) before stimulation and the tetanic tension recorded before ramp shortening (filled circles) are plotted (as ratios ofP_0) against initial fibre length (as a ratio of L_0, upper abscissa). The sarcomere length axis (lower abscissa) was constructed using the sarcomere lengths estimated by He–Ne laser diffraction for fibre lengths longer than ~L_0 (n = 16); a direct correlation between fibre length and sarcomere length was assumed. The lines and curves through the points are drawn by eye. The resting tension remains near zero until the fibre is lengthened beyond L_0 when it increases approximately exponentially (interrupted line). The slope of the tension decline after P_2 transition is plotted as P_0/s (open circles, right ordinate) in the upper panel. Note that the slope is negative in the plateau region of the force–length relation and becomes slightly positive at sarcomere lengths longer than ~2.80 μm (dotted vertical line); the resting tension is high at such longer lengths

10% L_0) at different initial fibre lengths and the pooled data are shown in Fig. 7. The post-P_2 tension rise during lengthening and the tension decline during shortening are seen over a wide range of initial fibre lengths. The rate of tension rise in lengthening remains similar at shorter fibre lengths and in the plateau region of the steady state force–length relationship, but increases markedly at fibre lengths greater than L_0. The tension decline data are basically similar to those in Fig. 6 except that due to the smaller amplitude of the ramp shortening, the definition of the slope was difficult and the slopes are lower and remain negative even at longer lengths. Since velocity was constant, the tension slope relates to ''stiffness'' and the stiffness is greater for lengthening than for shortening and it increases at longer fibre length; such estimates at longer sarcomere length, where there is appreciable resting tension, would of course be affected by passive tension changes.

Effect of caffeine on the tension responses to ramp shortening

Another possible cause of the tension decline after the P_2 transition during shortening is the shortening-induced deactivation (Edman 1975, 1980; Colomo et al. 1986); thus, shortening might interfere with the Ca-regulated, thin filament activating system (Eklund and Edman 1982). Therefore, as suggested to us by Professor Paul Edman (University of Lund, Sweden), we examined in separate experiments the effect of adding 0.5–5.0 mM caffeine to

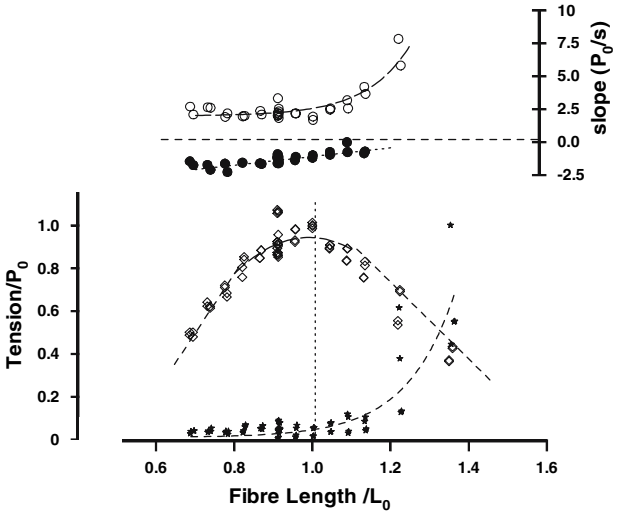

Fig. 7 The tension decline or rise after the P_2 transition at different fibre lengths. Pooled data from two fibre bundles showing the tetanic tension (open diamonds) and the resting tension (stars) at a range of fibre lengths; the presentation is similar to Fig. 6. Values for the tension slope during a standard ramp length step (velocity ~0.7 L_0/s, amplitude 10% L_0) are plotted as P_0/s, open circles for lengthening and filled circles for shortening; since velocity was constant, the tension slope relates to ''stiffness''. All lines through data points were fitted by eye. Note that the slope (stiffness) is greater for lengthening than for shortening and it increases substantially at longer fibre length

the Ringer solution: as shown in Fig. 8A, 2.5–5.0 mM caffeine clearly potentiated the isometric twitch tension but had only a minimal effect on the resting and tetanic tensions. We assumed that this is indicative of enhanced Ca-release during activation in the presence of caffeine without direct Ca-release by caffeine producing a significant contracture. Figure 8B shows superimposed tension responses to ramp shortening at a range of velocities at L_0 in the presence of caffeine; caffeine did not abolish the tension decline and the tension decline after P_2 remains clearly marked. Moreover, similar experiments on 5 preparations using 2.5–5 mM caffeine have shown that caffeine produced little if any change in the steady state force–shortening velocity relation determined as described in Fig. 2A. Data from one preparation are shown in Fig. 8C where the data with 5 mM caffeine (filled symbols) are superimposed on the control data, collected before caffeine and after recovery from caffeine (open symbols); the pooled data are given in Table 2. These data show that caffeine produced no significant effect on the steady state force–shortening velocity relation. In one experiment (see Fig. 8D), we examined the tension responses to a ramp shortening at different initial muscle fibre lengths and with and without 2.5 mM caffeine; the tension decline was seen and it decreased as the initial fibre length was made longer and became considerably less marked, or was absent, only at fibre lengths much longer than L_0.

Figure 9 shows the pooled data from the above experiments making a direct comparison of the rate of post-P_2 tension decline with caffeine and without caffeine. The analyses show that the (negative) slope of tension decline was slightly, but significantly, less in the presence of caffeine, particularly when compared with the control data after recovery from exposure to caffeine. Thus, our results indicate that there may be some degree of impairment of the Ca-activating system of the thin filament during shortening but, since it is not abolished by caffeine, it is unlikely to be the primary cause of the continued tension decline during shortening.

Tension response to a ramp length change during depression of active tension by BTS

In four experiments, we used *N*-benzyl-*p*-toluene sulphonamide (BTS) to depress the active force and examined the effect of this on the continued tension change during a ramp. BTS is a specific myosin inhibitor that suppresses crossbridge tension generation in muscle fibres (Cheung et al. 2002; Shaw et al. 2003); it does not affect the Ca-activation mechanisms in rat fibres and the force depression is accompanied by a reduction in rapid stiffness, i.e. it reduces the number of attached crossbridges (Pinniger et al. 2005). Figure 10A shows the tension response to stretch in the presence and absence of 10 μM BTS; in this preparation, the tetanic tension was reduced to <5% in the presence of BTS, but the continued tension rise during lengthening is still seen. Moreover, the slope of the tension rise remains 10–15 times higher than in resting fibres (see inset), essentially confirming our previous findings (Pinniger et al. 2006).

Since tension responses to ramp shortening were so small when the active force was reduced to such a low level, we used lower concentrations (5–7.5 μM) of BTS in three other experiments; Figure 10B shows experimental traces from one of them. The tension rise during lengthening and decline during shortening are seen when active tension is reduced to ~30–40%; the slopes of the tension changes, however, are reduced. In these experiments, the tension response to a standard ramp shortening was also recorded at different times after the saline flow to the chamber was changed to include BTS (see Methods), so that data could be collected at different reduced tension levels (see Fig. 11A); Fig. 11B (filled symbols; negative ordinate) shows the pooled data. It is seen that the slope of the tension decline decreases (becomes less negative) almost proportionately with BTS-induced tension depression, but remains negative over a large range of active force reduction (up to ~70%). The open symbols (positive ordinate) show individual measurements made with ramp lengthening in the same experiments (see Fig. 11 legend);

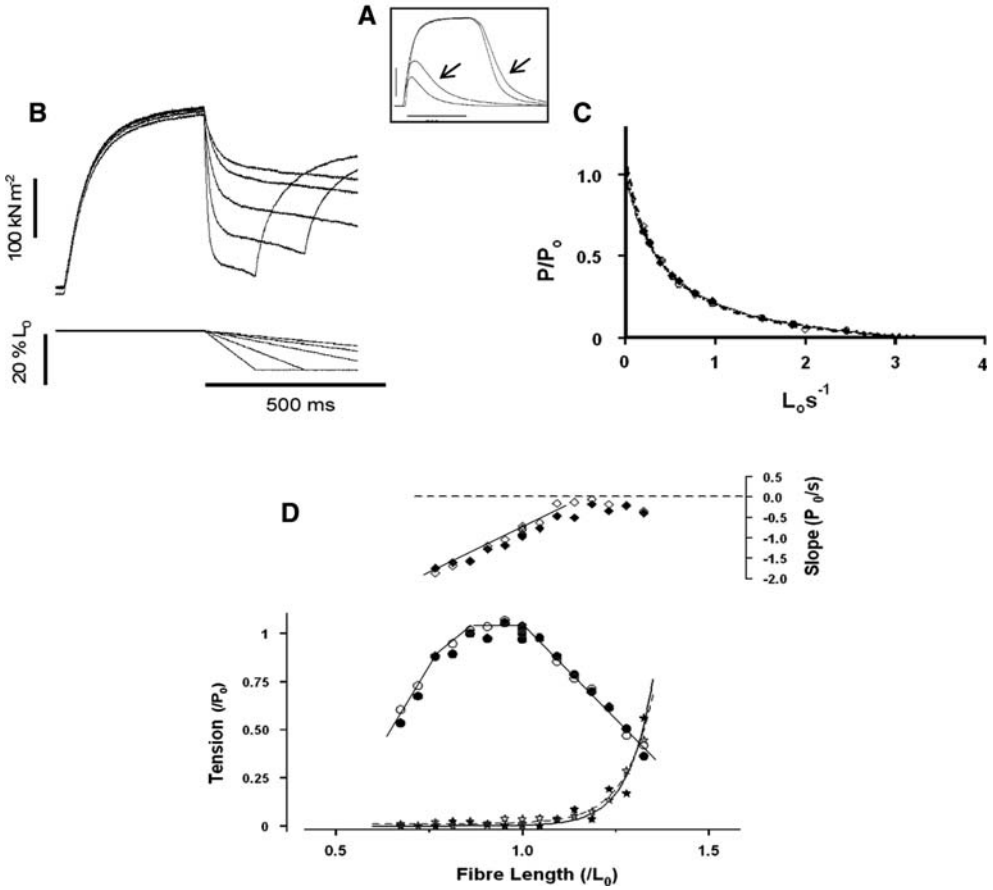

Fig. 8 Effects of caffeine on the shortening tension responses, the F–V relation and the force–length relation. **A**: (Inset) shows superimposed twitch and tetanic contractions from a preparation in the control bathing solution (no caffeine) and in a solution containing 2.5 mM caffeine (indicated by the arrows). With this level of caffeine, the twitch was potentiated but the tetanic tension was unaffected; the relaxation phase was slower. **B**: superimposed tension traces to ramp shortening from a preparation in the presence of 5 mM caffeine; the continued tension decline after the P_2 transition is clearly seen. An increase of tension decline is seen in the two higher velocity traces when the fibres shorten by >15% L_0; this is probably due to decreased filament overlap. **C**: A plot of the force at the P_2 transition versus shortening velocity, in controls before and after recovery from exposure to caffeine (open symbols, $n = 20$) and with 5 mM caffeine (filled symbols, $n = 10$); no obvious change in the force–velocity relation was noticeable with caffeine. **D**: Data from another experiment (presentation similar to Fig. 7) showing that the isometric force (lower panel) and the slope of post-P_2 tension decline during a ramp shortening (upper panel) at diferent fibre lengths are similar with and without caffeine; data with 2.5 mM caffeine are shown by the open symbols (lines are fitted by eye)

the slope of tension rise during lengthening is only reduced at low force levels. Thus, some deactivation may contribute to the tension decline in shortening and stiffening of non-crossbridge elements may be responsible for tension rise in lengthening.

Discussion

The tension response to ramp shortening or lengthening in tetanized rat muscle fibres showed two distinct transitions over a range of velocities. A transition P_2, identified by a

Table 2 Force–shortening velocity data under control conditions (without caffeine) and in the presence of 2.5 or 5 mM caffeine

	P_0 (kN m^{-2})	V_{max} (L_0/s)	a/P_0
Control ($n = 10$)	234 (±25.6)	3.30 (±0.59)	0.16 (±0.02)
With caffeine ($n = 5$)	234 (±17.0)	3.25 (±0.26)	0.15 (±0.01)

Mean (±s.e.m.) data from five fibre bundles at 20°C in which force and velocity measurements were made in the presence of caffeine, before exposure and after recovery from caffeine. The data were analysed as given in Table 1 and analysed control data before exposure to and after recovery from caffeine are pooled. The differences with and without caffeine are not significant ($P > 0.2$, paired t-test)

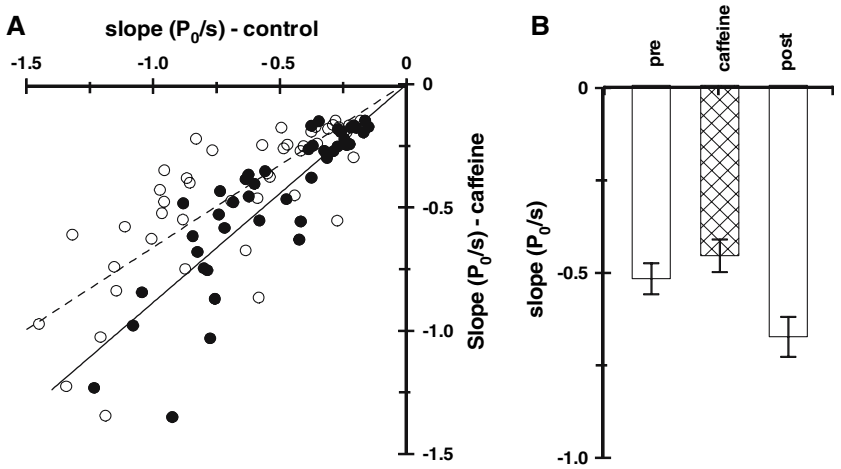

Fig. 9 Effects of caffeine on the tension decline during shortening. **A**: Data from 4 fibre bundles in which the rate of tension decline (negative linear slope) after the P_2 transition was determined at a number of shortening velocities in the presence of 2.5–5 mM caffeine; with the same velocities, the rate of tension decline was also determined in control solution. The rate with caffeine is plotted on the ordinate against the control rate obtained before (filled symbols and solid line) and after recovery from caffeine exposure (open symbols, dashed line) on the abscissa, lines are the linear regressions ($P < 0.01$). Note that compared to post-exposure control, the rate of tension decline is clearly less with caffeine (open symbols). **B**: Comparison of the mean (±s.e.m.) data for the rate of tension decline in control (open bars, pre-caffeine on the left) and in the presence of caffeine (cross-hatched bar). The differences between the means are significant (paired *t*-test, $P < 0.05$) indicating the rate of tension decline is decreased in the presence of caffeine; the decrease is much less when compared to the pre-caffeine control

gradual reduction in the rate of tension change, occurred at a change in length (L_2) of 14–28 nm/HS (half-sarcomere); the tension at this transition was used to construct the steady state force–velocity relation (see Figs. 2, 6). An earlier transition P_1 was observed (at ~1–3 ms) which became more apparent at higher velocities; the length change (L_1) at which this took place increased with velocity. The tension after the P_2 transition did not remain steady but continued to change until the end of the ramp. The present study is a systematic analysis of all these features. In the discussion below we consider that the P_1 and P_2 transitions, both during shortening and lengthening,

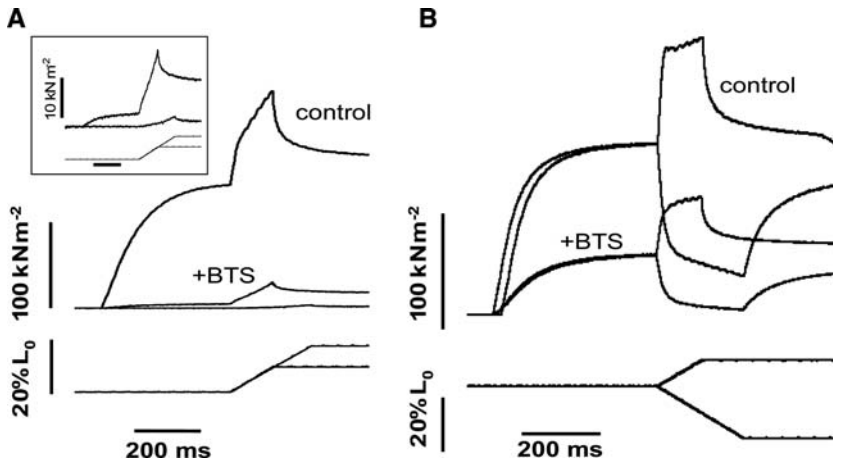

Fig. 10 Depression of active tension by BTS and the tension response to a ramp length change. **A**: Two tension responses from one preparation, before (control) and after exposure to 10 μM BTS (+BTS), are superimposed on the tension response in resting condition (bottom tension trace). The tetanic tension is reduced to <5% with BTS, but the tension rise during a lengthening ramp remains clear. (inset) The resting and active tension responses (with BTS) to stretch are shown on an amplified scale; the tension rise during lengthening in active muscle is 10–15 times larger than in resting muscle, although the latter was lengthened to twice the amplitude (velocity ~0.7 L_0/s). **B**: Traces from another preparation, showing tension responses to shortening and lengthening before and after exposure to 7.5 μM BTS. The continued tension rise during lengthening and tension decline during shortening are seen when the tetanic tension is reduced to ~30% with BTS; the slope however is reduced

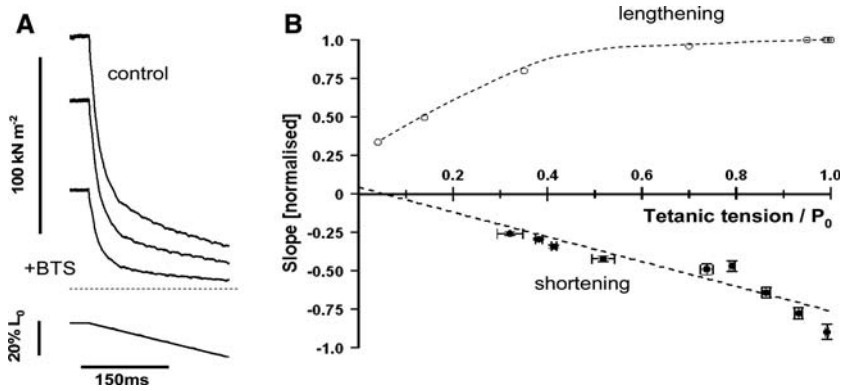

Fig. 11 Tension responses to ramp shortening during BTS inhibition. **A**: Sample traces from an experiment, where the tension response to a standard ramp shortening was recorded at regular intervals after normal saline flow to the chamber was replaced with 7.5 μM BTS saline. The control trace and two selected tension traces recorded at ~8 min and ~20 min after BTS flow began are shown. (Dashed line denotes zero tension level). **B**: Filled symbols show the pooled data collected from three experiments, similar to A; the slope of tension decline during ramp shortening (0.7–0.8 L_0/s) on being exposed to 7.5–10 μM BTS saline flow is plotted on a negative ordinate against the tetanic tension on the abscissa, both normalised to the respective control values. Each data point is mean (s.e.m.) of 4–8 measurements (total $n = 68$). Note that when isometric tension is reduced to ~30–40%, the continued tension decline during shortening (negative slope) is seen but its rate is decreased. Open symbols show individual measurements for the slope of tension rise ($n = 6$) during a ramp lengthening recorded from the same preparations once the BTS effect on force was steady; the rate of tension rise (positive slope) is decreased but to a much lesser extent than the decrease in tetanic tension

arise from crossbridge characteristics; the possible mechanisms for the continued tension change after the P_2 transition are discussed.

The P_1 transition

The attached crossbridges would be exposed to a change of strain during shortening or lengthening, but at the beginning of the ramp there would be no time for any steps in the crossbridge cycle to occur to an appreciable extent. So, ignoring the effects of end-compliance, the tension change at the start of the length step would be due to the sarcomeric compliance without the complexities of crossbridge attachment/detachment. The tension does not continue to change at this initial rate, but is interrupted by the inflection at the P_1 transition. In our previous study (Pinniger et al. 2006), we suggested that the P_1 transition during lengthening signals the rapid reversal of the power stroke in the post-stroke crossbridges as they become increasingly positively strained. Ford et al. (1977; see their Fig. 29) showed that the initial drop of tension during a *step* release and early recovery phase (T_1–T_2 transition) were also observable in the early stages of *ramp* shortening and represented by an inflection in the tension record. Hence, we interpret the P_1 transition during ramp shortening as reflecting the power stroke, i.e. the pre-stroke crossbridges undergoing the force-generating transition as they become increasingly negatively strained. The interpretation of the P_1 transition given above is in accordance with the Huxley–Simmons (1971) thesis for muscle force generation, formulated from analyses of the tension responses to small length steps; in brief, they proposed that a small release enhances force generation (by the power stroke) whereas a stretch reverses it. Various features of the P_1 transition (Figs. 3, 4) are consistent with this general concept; thus, the amplitude of P_1 and of L_1 increases with velocity, such that the stiffness at the P_1 transition is about the same in shortening as in lengthening, and is similar to the T_1 stiffness from length steps in the same muscle.

The P_2 transition

The P_2 transition represents the gradual transition to a new steady state in the crossbridge cycle where the filaments are sliding at a constant velocity. During lengthening, the extension L_2 at which the transition occurs remains similar (~14 nm/HS; Fig. 2B) at different velocities; during shortening, on the other hand, the magnitude of L_2 increases non-linearly with velocity and reaches a steady value of ~28 nm/HS at velocities higher than ~1 L_0/s. The muscle force measured at this transition was used to construct the F–V relation (see Fig. 2A). Since the force measured at the P_2 transition contains a contribution from the continued tension change, this is an approximate steady state F–V curve for the crossbridges; nevertheless, the present results are basically similar to the previous data from isotonic velocity measurement (see Table 1). The maximum filament sliding velocity for fast mammalian muscle at physiological temperatures would be greater than ~10 μm/s (per half-sarcomere), higher than the value (~8 μm/s at 35°C) estimated from in vitro motility assays (see Kawai et al. 2006).

Crossbridge modelling

By using a simple strain-dependent mechano-kinetic model based on the Lymn–Taylor scheme for the crossbridge cycle, shown here in Scheme 1, and simulating the force response to lengthening, we previously showed that reversal of the power stroke signalled the P_1 transition (Pinniger et al. 2006). The tension rose monotonically after the P_1 inflection and then levelled off at a half-sarcomere length increase (L_2) of ~14 nm, representing the P_2 transition. The modelling showed that the P_2 transition occurs when the occupancy of the original crossbridges—those attached at the beginning of lengthening—reaches very low levels (see Lombardi and Piazzesi 1990) and the switchover from original to newly attached crossbridges is essentially complete. Figure 12A shows that the same model can simulate the basic features of the tension response to shortening. Here, the early inflection at 1–3 ms marks the P_1 transition due to pre-stroke heads undergoing the power stroke. The P_2 transition occurs when half-sarcomere shortening (L_2) is ~17–18 nm, longer than the L_2 of 14 nm in the simulated lengthening tension response; although the absolute values are different, the longer L_2 during shortening is found experimentally. The simulation also shows that, at the P_2 transition, the switchover from original to newly attached crossbridges is essentially complete (Fig. 12A, D, E).

The simulated tension responses for both lengthening (Fig. 8 in Pinniger et al. 2006) and shortening (Fig. 12 in this paper) showed the basic features of the experimental tension responses, except for the continued tension change seen in the experimental records; we are continuing to improve the models but the simulations do not yet duplicate all the experimental features.

Some asymmetries between shortening and lengthening tension responses

The P_1 and P_2 transitions both showed some quantitative asymmetry between the lengthening and shortening limbs. For example, the time to the P_1 transition decreased with shortening velocity, but showed little decrease with lengthening velocity (Fig. 4A). Another aspect of this asymmetry is the apparent discontinuity about the isometric point between the times for the P_1 transition at low shortening velocities (~3 ms) and at low lengthening velocities (~2 ms). Similarly, in Fig. 2B, there is a marked difference between the shortening and lengthening limbs in the dependence of L_2 on velocity; L_2 increases with increasing shortening velocity to a plateau, whereas L_2 is constant in the lengthening limb. In our view, these asymmetries arise because different molecular events dominate during lengthening and shortening and because these events have different strain dependencies. At an early time during a lengthening ramp the P_1 transition occurs when some post-stroke heads undergo the reverse power stroke, whereas during a shortening ramp it occurs when pre-stroke heads execute the forward power stroke. At later times during lengthening, the P_2 transition occurs when the originally attached heads have largely detached by the reverse of step 1, while during shortening it occurs when the originally attached heads have largely detached by step 3. Since the rate constants for these four processes, and their sensitivities to strain, are different, the asymmetry of slope between shortening and lengthening limbs in Fig. 2B and Fig. 4A is understandable. It should be appreciated that in the velocity ramps the heads are exposed to greater positive or negative strains than are typically experienced in length step experiments. As discussed by Huxley and Simmons (1971) the rate of tension recovery after a length *step* is given by the sum of the rate constants for the forward and reverse power stroke. However, during *ramps* the strain is either continuously increasing (for lengthening) or continuously decreasing (for shortening). For example, whereas at the beginning of a shortening ramp the rate of re-equilibration between pre- and post-stroke heads may have a contribution from the reverse power stroke, this contribution would rapidly diminish in importance for all but the lowest velocities and the re-equilibration will be

Scheme 1 (Step-1 is attachment/detachment, step 2 is power stroke/reversal, step-3 is the irreversible step involving Pi-release, ATP binding and detachment and step 4 is ATP cleavage on detached heads)

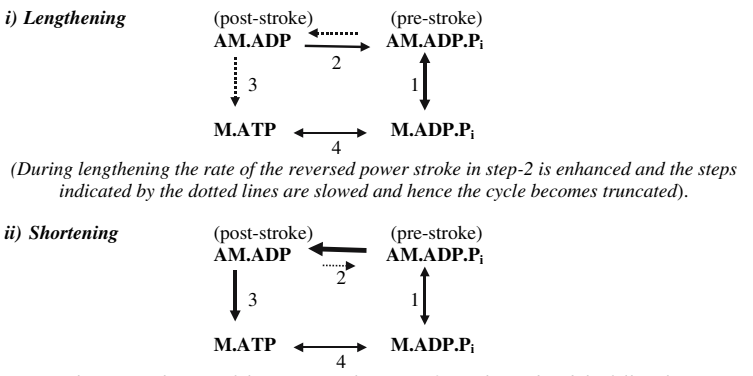

(During lengthening the rate of the reversed power stroke in step-2 is enhanced and the steps indicated by the dotted lines are slowed and hence the cycle becomes truncated).

(During shortening the rate of the power stroke in step-2 is enhanced and the full cycle operates faster).

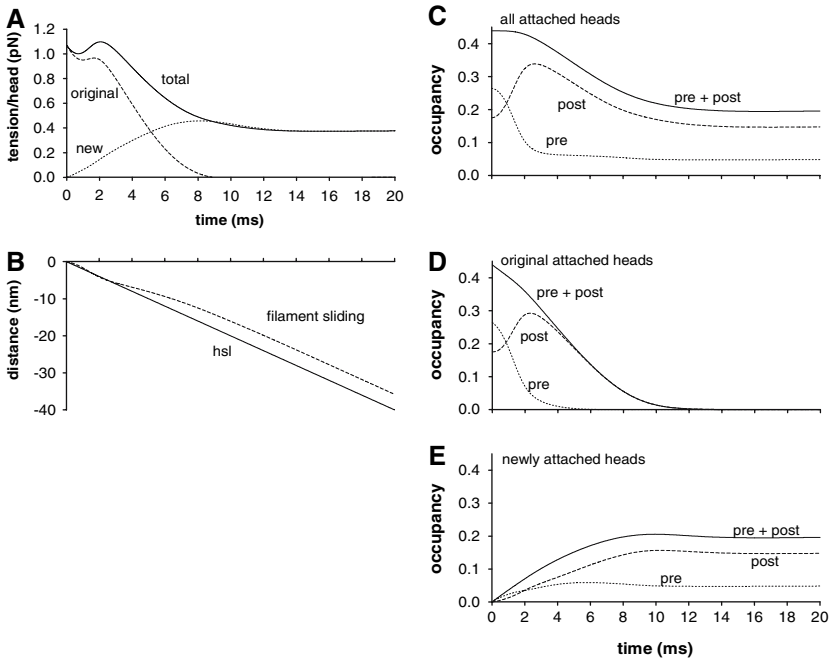

Fig. 12 Simulation of the tension transient during a ramp shortening using a model of the crossbridge cycle. The ramp shortening shown is 40 nm/h over 20 ms. **A:** Time-course of changes in tension expressed in pN head^{-1}. Continuous line is tension contribution from all attached heads (total); dashed line, contribution from heads that were attached at the beginning of the ramp (original) and dotted line, tension contribution from heads that become attached during the course of the ramp (new). **B**: Time-course of change (nm) in half sarcomere length (hsl) and distance of filament sliding (filament sliding). At the beginning of a ramp, there is no net detachment of heads (crossbidges) and tension is near isometric and, hence, the filament sliding is expected to lag behind hsl; however, due to other initial events (e.g. negative straining of compliance in filaments and crossbridges, power stroke etc.—see text), the filaments begin to lag behind later on and slide in parallel with hsl as the tension reaches a lower steady level. **C**: Time-course of changes in fractional occupancy of attached heads in the two conformations; pre + post, all attached heads; pre, pre-stroke conformation; post, post- stroke conformation. **D**: As **C** but considering only the heads that were attached at the beginning of the ramp. **E**: As **C** but considering only the heads that newly attach during the course of the ramp. The simulations were based on the Lymn-Taylor kinetic scheme for actomyosin ATPase in solution; the details of the model were described previously (Pinniger et al. 2006)

dominated by the increasing rate constant of the forward power-stroke. At very low velocities, just as in length steps, both processes may make significant contributions so that no discontinuity across the isometric point would be expected; however, establishing the continuity would require studying very low velocities where the transitions would be hard to observe.

The continued tension change during ramp lengthening and shortening

A continued tension rise during muscle fibre lengthening has been reported in several previous studies (Edman and Tsuchiya 1996; see references in Pinniger et al. 2006). The tension records during ramp shortening reported in mammalian muscles studies (e.g. Joyce et al. 1969, from cat [their Fig. 1a] and Asmussen and Marechal 1989, from rodents [their Fig. 1]) clearly show a continued tension decline after an initial fast decrease; Asmussen and Marechal (1989) indeed used an initial, small, length-release to unload series elasticity, but the tension decline was still seen during ramp shortening. Moreover, Joyce and Rack (1969) showed that, in the converse load-clamp experiment, the isotonic shortening velocity decreased significantly with time and that it could not be explained by changes in filament overlap. From the present study, the main features of the continuing tension change during a ramp are the following. Firstly, at a sarcomere length of ~2.5 μm (L_0), the tension continues to rise during lengthening or to decline during shortening at a rate that is velocity-sensitive; in shortening, the slope of tension decline reaches a steady value at velocities of 0.5–2 L_0/s (Fig. 5). The stiffness (slope/velocity) associated with the continuing tension is ~5–10 P_0/L_0 during lengthening and slow shortening, which is ~10% of the (rapid) crossbridge stiffness for this muscle at this temperature (see Pinniger et al. 2005); the stiffness is lower (<3 P_0/L_0) at moderate to high shortening velocities. Secondly, the continuing tension decline during shortening and tension rise during lengthening are found at the optimal sarcomere length range, and at lengths shorter and longer than optimal (Figs. 6, 7). Thirdly, the continued tension decline during

shortening was not abolished by caffeine indicating that it is not primarily due to Ca-sensitive thin filament de-activation (Fig. 9). Fourthly, the continued tension decline during a shortening is reduced, but not abolished, when the active force is depressed by BTS; the continued tension rise during lengthening is also reduced with BTS, but only at low force levels, and the stiffness remains much higher than in resting muscle.

The mechanisms that may contribute to a continuous tension change are the following. (1) *Stiffening of non-crossbridge elements*: Edman and Tsuchiya (1996) showed that during stretch of frog fibres the tension rise from the P_2 transition to the end of the ramp and the residual force enhancement after stretch are associated with strain building up in viscoelastic elements other than cross-bridges. We extended these findings to rat muscle (Pinniger et al. 2006) and proposed that this non-crossbridge contribution may arise from an increase upon activation of titin stiffness (see Labeit et al. 2003) and, possibly, from reversible binding of C-protein (Offer et al. 1973) to actin in a calcium-dependent manner (Moos 1981). It is also noteworthy that the existence of an increased non-cross-bridge stiffness in active muscle fibres has been demonstrated (Bagni et al. 2002, also see Fig. 10a), although its magnitude seems small. Such mechanisms, of course, will not alter the isometric active force versus sarcomere length relationship but they would contribute to tension changes when sarcomere length is changing. In principle, stiffening of non-crossbridge, visco-elastic elements can account for the continuing tension rise during stretch and tension decline during slow shortening at L_0 (see Fig. 5), their occurrence at a range of sarcomere lengths and, also, it may prevent sarcomere popping during lengthening. It is noteworthy that our modelling of the crossbridge cycle showed that, after the P_2 transition, the tension reaches a steady level and no further change in the distribution of strain in attached crossbridges occurs; this suggests that any further tension change observed after the P_2 transition has a non-crossbridge origin. (2) *Changes in filament overlap*: The increased rate of tension decline during shortening, particularly at shorter range of sarcomere lengths (Fig. 6), could be due to decrease in filament overlap. At longer sarcomere length, the continuing tension rise during a stretch was enhanced whereas the rate of tension decline during shortening was not much changed (Fig. 7); this might arise from the hysteresis in the force–extension relation and visco-elasticity that is also evident in resting muscle. (3) *Thin filament deactivation*: Our caffeine experiments suggest that changes in Ca-sensitive thin filament activation/deactivation (Fig. 8) is not the primary cause for the continued tension decline during shortening. On the other hand, Edman (1975) showed the occurrence of shortening deactivation and Colomo et al. (1986) showed a velocity-sensitive deactivation during muscle fibre shortening that may be Ca-insensitive; although the exact mechanism(s) remain unclear, the general implication was that changes in crossbridge cycling may interfere with thin filament activation/deactivation. Such mechanism(s) in combination may account for our finding that the slope of tension decline during ramp shortening was decreased with depression of active force, crossbridge attachments (Fig. 11). (4) *Sarcomere popping*: The continuing tension rise during a ramp stretch and the residual tension that persists afterwards have been attributed to increased sarcomere non-uniformity in muscle fibres and ''sarcomere popping'', i.e. lengthening of weak sarcomeres to beyond filament overlap, the tension in ''popped sarcomeres'' being then held by non-crossbridge elements (Morgan 1994). However, the latter idea has not received experimental support from recent experiments monitoring sarcomere and half sarcomere length changes during ramp stretch of myofibrils (Raisser et al. 2003; Telley et al. 2006); whereas the tension rise and residual tension were observed during and after a ramp stretch, there was no evidence of sarcomere popping; sarcomere heterogeneity was apparent but it did not increase during stretch. We used an intact fibre bundle preparation with short fibres (L_0 of ~2 mm) in which the tension responses were reproducible and the basic features seen at L_0; nevertheless, the possibility that segmental non-uniformities and series compliance may make some contribution to the tension behaviour during lengthening and shortening can not be entirely ruled out (see Julian and Morgan 1979; Edman and Reggiani 1984; Curtin and Edman 1989; Sugi and Tsuchiya 1988; Telley et al. 2003).

Thus, it appears that the continued tension rise during ramp lengthening may be due to stretch of non-crossbridge visco-elastic structures which stiffen on activation; also, release of tension in such structures is probably significant in slow ramp shortening. The tension decline during moderately fast ramp shortening, on the other hand, may in part be due to a form of Ca-insensitive de-activation of thin filament. The changes in sarcomere heterogeneity might contribute and modulate to varying extents these processes. Our experimental results show that continued tension change is a characteristic feature during lengthening and shortening in intact mammalian muscle; in so far that—within the force–velocity relation—the low velocities may be more physiologically relevant, the results indicate that stiffening of non-crossbridge elements would contribute significantly to energy storage (during lengthening) and release (during shortening) in active muscle in situ.

Acknowledgements We thank The Wellcome Trust for the support of our research and Professor Paul Edman (University of Lund, Sweden) for helpful suggestions on the work and comments on the manuscript.

References

Asmussen G, Marechal G (1989) Maximal shortening velocities, isomyosins and fibre types in soleus muscle of mice, rats and guinea-pigs. J Physiol 416:245–254

Bagni MA, Cecchi G, Colombini B, Colomo F (2002) A non-cross-bridge stiffness in activated frog muscle fibers. Biophys J 82:3118–3127

Bagni MA, Cecchi G, Colombini B, Colomo F (2005) Crossbridge properties investigated by fast ramp stretching of activated frog muscle fibres. J Physiol 565:261–268

Bressler BH (1985) Tension responses of frog skeletal muscle to ramp and step length changes. Can J Physiol Pharmacol 63:1617–1620

Cecchi G, Colomo F, Lombardi V (1978) Force-velocity relation in normal and nitrate-treated frog single muscle fibres during rise of tension in an isometric tetanus. J Physiol 285:257–273

Cecchi G, Colomo F, Lombardi V (1981) Force-velocity relation in deuterium oxide-treated frog single muscle-fibers during the rise of tension in an isometric tetanus. J Physiol 317:207–221

Cheung A, Dantzig JA, Hollingworth S, Baylor SM, Goldman YE, Mitchison TJ, Straight AF (2002) A small-molecule inhibitor of skeletal muscle myosin II. Nature Cell Biol 4:83–88

Colomo F, Lombardi V, Piazzesi G (1986) A velocity-dependent shortening depression in the development of the force-velocity relation in frog muscle fibres. J Physiol 380:227–238

Coupland ME, Ranatunga KW (2003) Force generation induced by rapid temperature jumps in intact mammalian (rat) skeletal muscle fibres. J Physiol 548:439–449

Curtin NA, Edman KAP (1989) Effects of fatigue and reduced intracellular pH on segment dynamics in isometric relaxation of frog-muscle fibres. J Physiol 413:159–174

Edman KAP (1975) Mechanical deactivation induced by active shortening in isolated muscle fibres of the frog. J Physiol 246:255–275

Edman KAP (1980) Depression of mechanical performance by active shortening during twitch and tetanus of vertebrate muscle fibres. Acta Physiol Sacnd 109:15–26

Edman KAP (1988) Double-hyperbolic force-velocity relation in frog muscle fibres. J Physiol 404:301–321

Edman KAP (2005) Contractile properties of mouse single muscle fibers, a comparison with amphibian muscle fibers. J Exp Biol 208:1905–1913

Edman KAP, Elzinga G, Noble MI (1978) Enhancement of mechanical performance by stretch during tetanic contractions of vertebrate skeletal muscle fibres. J Physiol 281:139–155

Edman KAP, Elzinga G, Noble MI (1981) Critical sarcomere extension required to recruit a decaying component of extra force during stretch in tetanic contractions of frog skeletal muscle fibres. J Gen Physiol 78:365–382

Edman KAP, Elzinga G, Noble MI (1982) Residual force enhancement after stretch of contracting frog single muscle fibres. J Gen Physiol 80:769–784

Edman KAP, Mulieri LA, Scuborn-Mulieri B. (1976) Non-hyperbolic force-velocity relationship in single muscle fibres. Acta physiol scand 98:143–156

Edman KAP, Reggiani C (1984) Redistribution of sarcomere length during isometric contraction of frog muscle fibres and its relation to tension creep. J Physiol 351:169–198

Edman KAP, Tsuchiya T (1996) Strain of passive elements during force enhancement by stretch in frog muscle fibres. J Physiol 490:191–205

Eklund MC, Edman KAP (1982) Shortening induced deactivation of skinned fibres of frog and mouse striated muscle. Acta Physiol Scand 116:189–199

Elmubarak MH, Ranatunga KW (1984) Temperature sensitivity of tension development in a fast-twitch muscle of the rat. Muscle Nerve 7:298–303

Flitney FW, Hirst DG (1978) Crossbridge detachment and sarcomere 'give' during stretch of active frog's muscle. J Physiol 276:449–465

Ford LE, Huxley AF, Simmons RM (1977) Tension responses to sudden length change in stimulated frog muscle fibres near slack length. J Physiol 269:441–515

Hill AV (1938) The heat of shortening and the dynamic constants of muscle. Proc Roy Soc Lond B 126:136–195

Huxley AF, Simmons RM (1971) Proposed mechanism of force generation in striated muscle. Nature 233:533–538

Jewell BR, Wilkie DR (1958) An analysis of the mechanical components in frog's striated muscle. J Physiol 143:5151–540

Joyce GC, Rack PM (1969) Isotonic lengthening and shortening movements of cat soleus muscle. J Physiol 204:475–491

Joyce GC, Rack PM, Westbury DR (1969) The mechanical properties of cat soleus muscle during controlled lengthening and shortening movements. J Physiol 204:461–474

Julian F, Morgan D (1979) The effect on tension of non-uniform distribution of length changes applied to frog muscle fibres. J Physiol 293:379–392

Kawai M, Kido T, Vogel M, Fink RHA, Ishiwata S (2006) Temperature change does not affect force between regulated actin filaments and heavy meromyosin in single-molecule experiments. J Physiol 574:877–887

Labeit D, Watanabe K, Witt C, Fujita H, Wu Y, Lahmers S, Funck T, Labeit S, Granzier H (2003) Calcium-dependent molecular spring elements in the giant protein titin. PNAS 100:13716–13721

Lombardi V, Piazzesi G (1990) The contractile response during steady lengthening of stimulated frog muscle fibres. J Physiol 431:141–171

Lymn RW, Taylor EW (1971) Mechanism of adenosine triphosphate hydrolysis by actomyosin. Biochem 10:4617–4624

Månsson A (1994) The tension response to stretch of intact skeletal muscle fibres of the frog at varied tonicity of the extracellular medium. J Muscle Res Cell Motil 15:145–157

Moos C (1981) Fluorescence microscope study of the binding of added C protein to skeletal muscle myofibrils. J Cell Biol 90:25–31

Morgan DL (1994) An explanation for residual increased tension in striated muscle after stretch during contraction. Exp Physiol 79:831–838

Morgan DL, Clafflin DR, Julian FJ (1991) Tension as a function of sarcomere length and velocity of shortening in single skeletal muscle fibres of the frog. J Physiol 441:719–732

Mutungi G, Ranatunga KW (2000) Sarcomere length changes during end-held (isometric contractions in intact mammalian (rat) fast and slow muscle fibres. J Muscle Res Cell Motil 21:565–575

Mutungi G, Ranatunga KW (2001) The effects of ramp stretches on active contractions in intact mammalian fast and slow muscle fibres. J Muscle Res Cell Motil 22:175–184

Offer G, Moos C, Starr R (1973) A new protein of the thick filaments of vertebrate skeletal myofibrils. Extraction, purification and characterization. J Mol Biol 74:653–676

Piazzesi G, Francini F, Linari M, Lombardi V (1992) Tension transients during steady lengthening of tetanized muscle fibres of the frog. J Physiol 445:659–711

Pinniger GJ, Bruton JD, Westerblad H, Ranatunga KW. (2005) Effects of a myosin-II inhibitor (*N*-benzyl-*p*-toluene sulphonamide, BTS) on contractile characteristics of intact fast-twitch mammalian muscle fibres. J Mus Res Cell Motil 26:135–141

Pinniger GJ, Ranatunga KW, Offer GW (2006) Crossbridge and non-crossbridge contributions to tension in lengthening muscle:

force-induced reversal of the power stroke. J Physiol 573:627–643

Ranatunga KW (1984) The force-velocity relation of rat fast- and slow-twitch muscles examined at different temperatures. J Physiol 351:517-529

Rassier DE, Herzog W, Pollack GH (2003) Stretch-induced force enhancement and stability of skeletal muscle myofibrils. Adv Exp Med Biol 538:501–515

Roots HR, Ranatunga KW (2005) Tension responses to ramp shortening in tetanized intact rat muscle fibres. J Physiol 567P:123P

Roots HR, Ranatunga KW (2006) Tension responses to ramp shortening in tetanized rat muscle fibres: effects of caffeine. Proc Physiol Soc 3:PC103

Shaw MA, Ostap EM, Goldman YE (2003) Mechanism of inhibition of skeletal muscle actomyosin by N-benzyl-p-toluene sulfonamide. Biochemistry 42:6128–6135

Stienen G, Versteeg P, Papp Z, Elzinga G (1992) Mechanical properties of skinned rabbit psoas and soleus muscle fibres during lengthening: effects of phosphate and Ca2+. J Physiol 451:503–523

Sugi H, Tsuchiya T (1988) Stiffness changes during enhancement and deficit of isometric force by slow length changes in frog skeletal muscle fibres. J Physiol 407:215–229

Telley A, Denoth J, Ranatunga KW (2003) Inter-sarcomere dynamics in muscle fibres: a neglected subject? Adv Exp Med Biol 538:481–500

Telley A, Stehle R, Ranatunga KW, Pfitzer G, Stüssi E, Denoth J (2006) Dynamic behaviour of half-sarcomeres during and after stretch in activated psoas myofibrils: sarcomere asymmetry but no ''sarcomere popping. J Physiol 573:173–185

ter Keurs HE, Luff AR, Luff SE (1984) Force-sarcomere-length relation and filament length in rat extensor digitorum muscle. Adv Exp Med Biol 170:511–525